

## Magnon-fracton crossover in quenched random site-diluted ferromagnets

S. N. Kaul\* and S. Srinath

School of Physics, University of Hyderabad, Central University P.O., Hyderabad 500 046, Andhra Pradesh, India

(Received 9 October 2000; published 6 February 2001)

The strong departure from the Bloch  $T^{3/2}$  law behavior of magnetization in dilute amorphous  $(T_p\text{Ni}_{1-p})_{80}\text{B}_{16}\text{Si}_4$  ( $T=\text{Fe,Co}$ ) alloys is shown to be a manifestation of the crossover from hydrodynamic to critical spin wave dynamics induced by the diverging correlation length near percolation threshold. An appropriate choice of the density of states for magnetic excitations on self-similar (fractal) percolation network permits an accurate determination of the magnon-to-fracton crossover line in the magnetic phase diagram of quenched random site-diluted ferromagnets. By unambiguously demonstrating that the fracton dimensionality  $\tilde{d}_f \approx 4/3$  and the conductivity percolation critical exponent  $\sigma_p < 2$ , the present results vindicate the Alexander-Orbach conjecture and the Golden inequality for percolating network with Euclidean dimension  $d=3$ .

DOI: 10.1103/PhysRevB.63.094410

PACS number(s): 75.40.Gb, 64.60.Ak, 75.30.Ds

### I. INTRODUCTION

Considerable effort has lately<sup>1</sup> gone into understanding the nature of quantized excitations in fractal networks, the crossover between extended (phonon, magnon) and strongly localized (fracton) excitations, and the effect of this crossover on thermodynamic and transport properties of random physical systems. One of the early attempts to determine the density of states and the dispersion relation for vibrational excitations of a  $D_f$ -dimensional fractal network is due to Alexander and Orbach<sup>2</sup> who termed such excitations as *fractons* and conjectured that fracton dimensionality  $\tilde{d}_f = 4/3$  for percolation networks with Euclidean dimension  $d \geq 2$ . Recent large-scale (hence most accurate) numerical simulations<sup>1</sup> yield estimates for  $\tilde{d}_f$  that are close to  $4/3$  only for  $d=2$  but substantially deviate from  $4/3$  for  $d=3$ . Besides this discrepancy, the major factor responsible for slowing down the progress in this field of research is the observation that many theoretical predictions still await rigorous experimental confirmation, as elucidated below.

One of the well-known realizations of a self-similar (fractal) network is a quenched random site-diluted Heisenberg magnet with the concentration of magnetic atoms ( $p$ ) near the percolation threshold ( $p_c$ ). At  $p=p_c$ , an *infinite* magnetic cluster first appears (such that for  $p < p_c$ , only finite magnetic clusters are present and no long-range magnetic order exists even for temperatures as low as  $T=0$  K) and the percolation correlation length at  $T=0$  K,  $\xi_0(p)$ , diverges in accordance with the relation<sup>3</sup>

$$\xi_0(p) = \xi_p (p - p_c)^{-\nu_p}. \quad (1)$$

The divergence in  $\xi_0(p) \equiv \xi(T=0, p)$  induces a crossover in the dynamics of Heisenberg spins from hydrodynamic behavior for  $k\xi < 1$  to critical behavior for  $k\xi > 1$ , where  $k$  is the inverse wavelength of spin waves in the hydrodynamic regime and the inverse characteristic length of the localized fracton modes in the critical regime. A change from Euclidean dimension  $d$  to fractal dimension  $D_f$  results in a crossover in the dispersion relation and density of states from long-wavelength, low-frequency ( $\omega \ll \omega_{co}$ ) magnons (*hydrodynamic*) to short-length-scale, high-frequency ( $\omega \gg \omega_{co}$ )

magnetic fracton (*critical*) forms at a characteristic frequency  $\omega_{co}$ . Such a crossover not only substantially alters the functional dependence of magnetization on temperature,  $M(T)$ , but affects other static thermal properties also. This crossover is different from the usual thermal-to-percolation crossover<sup>3</sup> which occurs when the thermal fluctuations of the order parameter become *critical* at a *concentration-dependent* temperature  $T_C(p)$  as the percolation critical point  $Q(p=p_c, T=0)$  is approached along the path  $T \rightarrow 0$  at  $p \approx p_c$ . For a given concentration,  $T_C(p)$  represents the temperature at which a transition from the paramagnetic state to ferromagnetic (or antiferromagnetic) state takes place when the temperature is lowered from high temperatures.

To date, only two attempts<sup>4,5</sup> have been made to experimentally determine the theoretically expected<sup>1,6</sup> fracton contribution to  $M(T)$  in site-diluted amorphous ferromagnets with  $p \geq p_c$ . Besides yielding widely different values<sup>4,5</sup> for  $\tilde{d}_f$ , such studies suffer from a number of major flaws. These include the following: (i) contrary to the claim made by Salamon and Yeshurun,<sup>4</sup> the expression for the density of states used does not yield the correct asymptotic form in the fracton regime, (ii) the magnon-to-fracton crossover frequency  $\omega_{co}$  was considered to be independent of the external magnetic field, and (iii) the temperature renormalization of spin-wave stiffness was not taken into account. Thus, the reported<sup>4,5</sup> agreement between theory and experiment is fortuitous. Some evidence<sup>7</sup> for antiferromagnetic fractons has recently been provided by inelastic neutron scattering data taken on a diluted Heisenberg antiferromagnet.

By subjecting the theoretical predictions<sup>1,2,6</sup> to the most rigorous experimental test, the results reported in this paper provide, by far, the strongest evidence for the occurrence of magnon-to-fracton crossover in quenched random site-diluted ferromagnets and testify to the validity of the Alexander-Orbach conjecture (Golden inequality) that  $\tilde{d}_f = 4/3$  (the conductivity exponent  $\sigma \leq 2$ ) for  $d=3$ . Moreover, the present results permit an accurate determination of the hydrodynamic-to-critical spin-wave crossover line in the magnetic phase diagram and clearly bring out the functional forms of the magnetic field dependence of the crossover frequency  $\omega_{co}$  as well as the temperature dependence of the spin-wave stiffness.

## II. EXPERIMENTAL DETAILS

Magnetization ( $M$ ) of the well-characterized<sup>8</sup> chemically homogeneous amorphous  $(a)(\text{Fe}_p\text{Ni}_{1-p})_{80}\text{B}_{16}\text{Si}_4$  ( $p = 0.0540, 0.0875, 0.1125, 0.1375$ ) and  $(\text{Co}_{p'}\text{Ni}_{1-p'})_{80}\text{B}_{16}\text{Si}_4$  ( $p' = 0.1125, 0.1375, 0.2375$ ) alloys with composition  $(p, p')$  near the percolation threshold [ $p_c = 0.0285(5)$ ,  $p'_c = 0.0684(4)$ ] for the appearance of long-range ferromagnetic order was measured as a function of the external magnetic field ( $H$ ) at  $T = 3.8$  K in fields up to 70 kOe and as a function of temperature at  $H = 2.5, 5.0, 7.5,$  and  $10.0$  kOe in the temperature range  $5 \text{ K} \leq T \leq 2T_C$  ( $T_C =$  Curie point) with a relative accuracy of better than 10 ppm using a superconducting quantum interference device (SQUID) magnetometer. The demagnetizing factor  $N$  for each composition was determined<sup>8</sup> from low-field ( $\leq 20$  Oe) magnetization data. In these alloy systems, Ni atoms carry small<sup>9</sup> or even no magnetic moment and hence act as magnetic dilutents. The above choice of  $H$  values is dictated by the requirement that the field strength be high enough to completely wipe out the irreversibility observed<sup>10</sup> in the low-field magnetization (which is an attribute of the reentrant behavior at low temperatures in the alloys with  $p < 0.1$  or  $p' < 0.2$ ) but not so large as to completely suppress the spin waves.

## III. DATA ANALYSIS, RESULTS, AND DISCUSSION

The Curie temperature  $T_C$  for all the compositions in the presently investigated alloy series has recently been accurately determined by an elaborate analysis<sup>8</sup> of the ‘‘zero-field’’ susceptibility in the critical region near the ferromagnetic (FM) to paramagnetic (PM) phase transition. By least-squares fitting the  $T_C(p)$  data to the expression<sup>3</sup>

$$T_C(p) = t_p(p - p_c)^\phi, \quad (2)$$

with  $t_p$ ,  $p_c$ , and  $\phi$  as free parameters (Fig. 1), the thermal-to-percolation crossover exponent  $\phi$  is estimated to be  $\phi = 1.10(2)$  [ $\phi = 1.14(4)$ ] and  $p_c = 0.0282(2)$  [ $p'_c = 0.0685(2)$ ]. Spontaneous magnetization at 0 K (in Gauss) for each composition,  $M_0(p) \equiv M(T=0, p)$ , is obtained as an intercept on the ordinate when the *linear* high-field portion of the  $M$ - $H$  isotherm taken at  $T = 3.8$  K is extrapolated to  $H = 0$ . The expression<sup>3</sup>

$$M_0(p) = m_p(p - p_c)^{\beta_p} [1 + a(p - p_c)^\Delta], \quad (3)$$

predicted by the percolation theory, with  $\Delta = 1.0$  and the parameter values  $m_p = 839(1)G$  [ $m_{p'} = 304(1)G$ ],  $\beta_p = 0.41(1)$  [ $\beta_{p'} = 0.41(1)$ ], and  $p_c = 0.0288(2)$  [ $p'_c = 0.0682(2)$ ], is found to closely reproduce (solid curves in Fig. 1) the observed concentration dependence (symbols in Fig. 1) of  $M_0$ . In Eq. (3),  $\beta_p$  is the percolation critical exponent,  $a$  and  $\Delta$  are the ‘‘correction-to-scaling’’ amplitude and exponent, respectively. Note that the correction term in Eq. (3) is very (not so) important in Co (Fe) containing alloys. The presently determined values of  $\phi$  and  $\beta_p$  are in perfect agreement with not only those previously determined<sup>11</sup> by us for other amorphous systems but also with the theoretically predicted ones.<sup>1,3</sup>

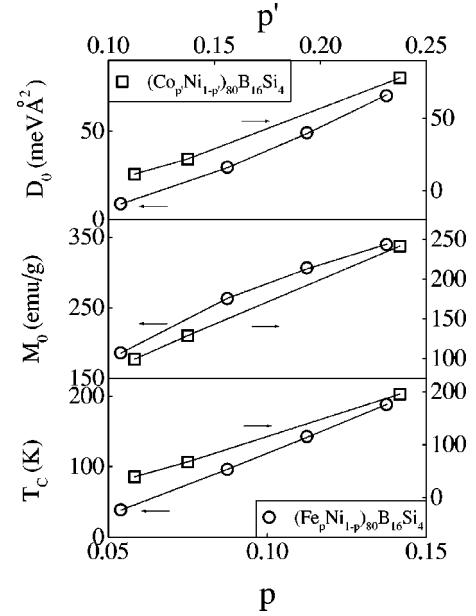


FIG. 1. Variation of  $T_C(p)$  [ $T_C(p')$ ],  $M(T=0, p)$  [ $M(T=0, p')$ ] and  $D_0(T=0, p)$  [ $D_0(T=0, p')$ ] with Fe [Co] concentration  $p$  [ $p'$ ]. The solid curves through the data points (open symbols) represent the least-squares fits to the data based on Eqs. (2), (3), and (20), respectively. Horizontal arrows indicate the relevant ordinate scales.

In case spin-wave excitations are solely responsible for thermal demagnetization, a plot of ‘‘in-field’’ magnetization versus  $T^{3/2}$  is expected to exhibit a *concave downward* curvature due to (i) the presence of higher-order terms in the magnon dispersion relation, (ii) the temperature renormalization of the spin-wave stiffness, and (iii) the gap in the spin-wave spectrum introduced by  $H$  and other anisotropy fields. Contrary to this expectation, a marked *concave upward* curvature is observed in the  $M$ - $T^{3/2}$  curves regardless of the alloy composition (Fig. 2 depicts one such plot); this curvature becomes more pronounced as  $p \rightarrow p_c$  ( $p' \rightarrow p'_c$ ). The departure from the expected behavior is indicative of the presence of an additional contribution to  $M(T, H)$  due to ferromagnetic fractons. To incorporate this additional contribution properly, we adopt the following approach.

The general scaling form<sup>12</sup> for the density of vibrational states of a percolating network for  $p > p_c$  is

$$N(\omega) = A \omega^{x-1} f(\omega/\omega_{co}), \quad (4)$$

where  $x$  is the fracton dimensionality whose explicit expression depends on the particular fractal model chosen,  $\omega_{co}$  is the frequency at which a crossover occurs from hydrodynamic (phonon or magnon) regime to the critical (fractal) regime, and  $A$  is a constant *independent* of  $\omega_{co}$ . The scaling function  $f(z)$  in Eq. (4) has the asymptotic limits  $f(z) \rightarrow 1$  as  $z \rightarrow \infty$  and  $f(z) \rightarrow z^{d'-x}$  as  $z \rightarrow 0$  so that<sup>12</sup>

$$N_{hy}(\omega) = A \omega_{co}^{x-d'} \omega^{d'-1} \quad (5)$$

in the hydrodynamic ( $\omega \ll \omega_{co}$ ) limit and

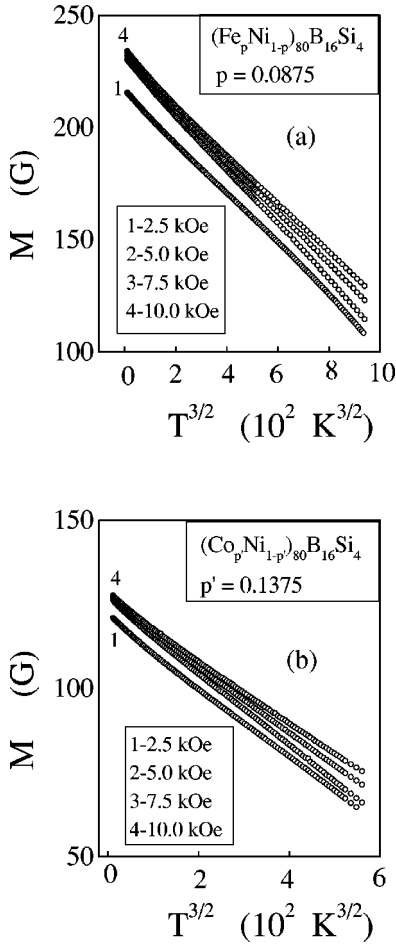


FIG. 2.  $M(T, H)$  is plotted against  $T^{3/2}$  in order to highlight the concave upward curvature for the alloy with (a)  $p=0.0875$  in  $a-(\text{Fe}_p \text{Ni}_{1-p})_{80} \text{B}_{16} \text{Si}_4$  alloy series and (b)  $p'=0.1375$  in  $a-(\text{Co}_p \text{Ni}_{1-p'})_{80} \text{B}_{16} \text{Si}_4$  alloy series.

$$N_{cr}(\omega) = A \omega^{x-1} \quad (6)$$

in the critical ( $\omega \gg \omega_{co}$ ) limit. In the case of phonon-fracton (magnon-fracton) crossover, the fracton dimensionality  $x$  and the dimension  $d'$  are<sup>1</sup>  $x = \tilde{d}$  ( $x = \tilde{d}_f/2$ ) and  $d' = d$  ( $d' = d/2$ ), respectively. Salamon and Yeshurun<sup>4</sup> have suggested the following expression for the effective density of states (DOS) in  $d=3$  percolating ferromagnetic networks:

$$N_{eff}(\omega) = (1/4\pi^2) [\hbar/D(p)]^{d/2} \omega^{(d/2)-1} \left(1 + \frac{\omega}{\omega_{co}}\right)^{(\tilde{d}_f-d)/2}, \quad (7)$$

where  $D(p)$  is the concentration-dependent spin-wave (SW) stiffness and  $\tilde{d}_f$  is the ferromagnetic fracton dimensionality. In the limits  $\omega \ll \omega_{co}$  and  $\omega \gg \omega_{co}$ , Eq. (7) reduces to

$$N_{SW}(\omega) = A' \omega_{co}^{d[(\tilde{d}_f/D_f)-1]/2} \omega^{(d/2)-1} \quad (8)$$

and

$$N_{fr}(\omega) = A' \omega_{co}^{\tilde{d}_f[(d/D_f)-1]/2} \omega^{(\tilde{d}_f/2)-1}, \quad (9)$$

respectively, with  $A' = (1/4\pi^2) \{\hbar \omega_p^{1-(\tilde{d}_f/D_f)}/d_p\}^{d/2}$ . In arriving at Eqs. (8) and (9), use has been made of the following relations:<sup>1</sup>

$$D(p) = d_p (p - p_c)^{2\nu_p[(D_f/\tilde{d}_f)-1]} \quad (10)$$

and

$$\omega_{co}(p) = \omega_p (p - p_c)^{2\nu_p D_f/\tilde{d}_f}. \quad (11)$$

A comparison between the asymptotic limits of the DOS expression, Eq. (7), and those of the general scaling expression for DOS, Eq. (4), reveals the following. (i) Notwithstanding the difference in the exponent of  $\omega_{co}$ , Eqs. (8) and (5) are similar in form. (ii) Contrary to the theoretical expectation,<sup>1,12</sup> i.e., Eq. (6), the prefactor of the term  $\omega^{x-1}$  in Eq. (9) depends on  $\omega_{co}$ . Thus, Eq. (7), at best, predicts a correct asymptotic form in the magnon limit *but not* in the fracton limit. To remedy this flaw, we propose the density of states of the form

$$n_{eff}(\omega) = (p - p_c)^{\nu_p(D_f-d)} N_{eff}(\omega) = (1/4\pi^2) [\hbar/D(p)]^{d/2} \times (p - p_c)^{\nu_p(D_f-d)} \omega^{(d/2)-1} \left(1 + \frac{\omega}{\omega_{co}}\right)^{(\tilde{d}_f-d)/2}, \quad (12)$$

with  $N_{eff}(\omega)$  given by Eq. (7). Unlike the form of DOS proposed earlier,<sup>4</sup> Eq. (12) yields the correct asymptotic forms<sup>1,12,13</sup>

$$n_{SW}(\omega) = A'' \omega_{co}^{(\tilde{d}_f-d)/2} \omega^{(d/2)-1} \quad (13)$$

and

$$n_{fr}(\omega) = A'' \omega^{(\tilde{d}_f/2)-1}, \quad (14)$$

with  $A'' = (1/4\pi^2) \{\hbar \omega_p^{1-(\tilde{d}_f/d)}/d_p\}^{d/2}$ , in the magnon ( $\omega \ll \omega_{co}$ ) [cf. Eqs. (5) and (13)] and fracton ( $\omega \gg \omega_{co}$ ) [cf. Eqs. (6) and (14)] regimes, and ensures a smooth crossover between the two regimes at  $\omega = \omega_{co}$ . Consequently, the ratio  $n_{fr}(\omega_{co})/n_{SW}(\omega_{co}) = a$  is a constant independent<sup>11</sup> of  $\omega_{co}$  (i.e., the ratio is noncritical). To facilitate the computation of magnetization at finite fields and temperatures, Eq. (12) is cast into an alternative form

$$n_{eff}(\omega) = (1/4\pi^2) [\hbar/D(p)]^{d/2} [m_p^*/M_0(p)] \omega^{(d/2)-1} \times \left(1 + \frac{\omega}{\omega_{co}}\right)^{(\tilde{d}_f-d)/2} \quad (15)$$

by making use of the relation<sup>1,6</sup>

$$D_f = d - (\beta_p/\nu_p) \quad (16)$$

and Eq. (3). In Eq. (15),  $m_p^* = m_p [1 + a(p - p_c)^\Delta]$ .

The magnetization  $M(T, H)$  is calculated by numerically integrating over the density of states,  $n_{eff}(\omega)$ , Eq. (15), and using the Bose-Einstein function, which accounts for the gap introduced in the spin-wave spectrum by the effective field

$H_{eff} = H - H_d + H_A$  (where  $H_d = 4\pi NM$  and  $H_A$  are the demagnetizing and uniaxial anisotropy fields,<sup>14</sup> respectively):

$$M(T, H) = M(0, H) - g\mu_B \int_0^\omega \frac{n_{eff}(\omega) d\omega}{e^{(\hbar\omega + g\mu_B H_{eff})/k_B T} - 1}. \quad (17)$$

The calculated values of  $M(T, H)$  do not depend on the upper integration limit  $\omega$  when  $\omega > 10^{13}$  Hz. At any given value of  $H$ , the agreement between the observed and calculated values of  $M$  at different temperatures  $T \leq T_C$  is optimized, at first, by keeping  $\tilde{d}_f$  fixed at values differing by 0.01 in the range  $1.2 \leq \tilde{d}_f \leq 1.4$  and varying  $M(0, H)$ ,  $D$ , and  $\omega_{co}$ . When this exercise yields the optimum values of  $\tilde{d}_f$  and  $M(0, H)$  as  $\tilde{d}_f = 1.33(3)$  and  $M(0, H) = M(3.8 \text{ K}, H)$ ,  $\tilde{d}_f$  and  $M(0, H)$  are kept constant at these values in the subsequent fits. The optimization process reveals that the quality of fits, based on Eq. (17), improves considerably if the temperature dependence of the spin-wave stiffness  $D$  is taken into account. Out of the relations<sup>14</sup>

$$D(T) = D_0 (1 - D_{5/2} T^{5/2}) \quad (18)$$

and

$$D(T) = D_0 (1 - D_2 T^2), \quad (19)$$

predicted, respectively, by the Heisenberg (localized-electron) and itinerant-electron models for the thermal renormalization of  $D$ , Eq. (18) reproduces the  $M(T, H)$  data more closely, as is evident from a typical plot of the percentage deviation of the experimental data from the best least-squares fits, based on Eqs. (18) and (19), shown in Fig. 3. From the optimum fit (illustrated by the solid curves through the data points in Fig. 4), the parameters  $D_0(p) \equiv D(T=0, p)$ ,  $D_{5/2}$ , and  $\omega_{co}$  at a given value of  $H$  are determined for each composition. Irrespective of  $H$ , the power laws<sup>1</sup>

$$D_0(p) = d_p (p - p_c)^{\theta_p}, \quad (20)$$

with  $p_c = 0.0285(2)$  [ $p'_c = 0.0686(2)$ ] and  $\theta_p = 2\nu_p [(D_f/\tilde{d}_f) - 1] = 1.45(2)$  [1.45(3)], and

$$\omega_{co}(p) = \omega_p (p - p_c)^{\theta_p + 2\nu_p}, \quad (21)$$

with  $p_c = 0.0286(2)$  [ $p'_c = 0.0684(3)$ ] and  $\theta_p + 2\nu_p = 3.17(2)$  [3.17(3)], describe the  $D_0(p)$  and  $\omega_{co}(p)$  data quite well (Figs. 1 and 5). At this stage, it is gratifying to note that different sets of data, i.e.,  $T_C(p)$ ,  $M_0(p)$ ,  $D_0(p)$ , and  $\omega_{co}(p)$ , all yield the same value for the critical concentration  $p_c$ , within the uncertainty limits, for a given alloy series. While the quantities  $D_0$ ,  $d_p$ ,  $\theta_p$ , and  $\theta_p + 2\nu_p$  are independent of  $H$ ,  $D_{5/2}$ ,  $\omega_{co}$ , and  $\omega_p$  decrease with increasing  $H$  for a given composition. That the observed field dependence of  $\omega_{co}$  is closely reproduced by the empirical relation

$$\omega_{co}(H) = a [1 + b e^{-H/H^*}] \quad (22)$$

is clearly borne out by the optimum fits (solid curves) to the  $\omega_{co}(H)$  data (open circles), based on Eq. (22) and displayed

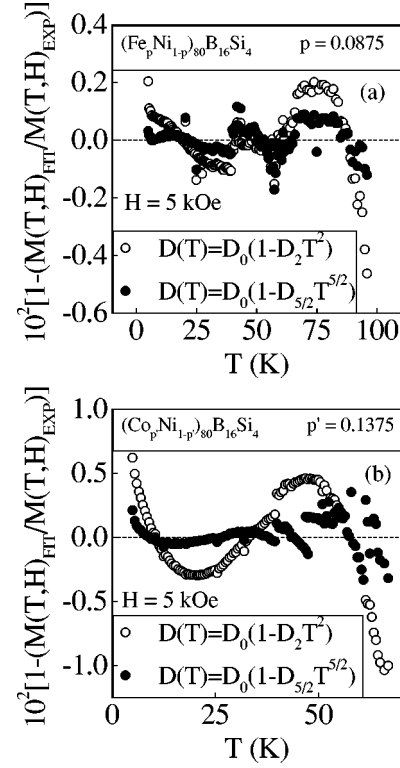


FIG. 3. Temperature variations of the percentage deviation of the  $M(T, H=5 \text{ kOe})$  data from the optimum fits based on Eqs. (17) and (18) or (17) and (19) of the text for the alloy with (a)  $p = 0.0875$  in  $a\text{-(Fe}_p\text{Ni}_{1-p})_{80}\text{B}_{16}\text{Si}_4$  series and (b)  $p' = 0.1375$  in  $a\text{-(Co}_{p'}\text{Ni}_{1-p'})_{80}\text{B}_{16}\text{Si}_4$  series.

in Fig. 6. The effect of the field is to suppress spin-wave excitations and to induce long-range correlations between spins. As a result of the reduction in the number of magnons and the increase in  $\xi_0$  with increasing  $H$ ,  $D_{5/2}$  (which is a measure of the strength of magnon-magnon interactions<sup>14</sup>) and  $\omega_{co}(p, H) \sim D_0(p) / [\xi_0(p, H)]^2$  both diminish.

From the values of  $\omega_{co}$  at different fields for each composition,  $\omega_{co}$  at zero field,  $\omega_{co}(0)$ , is calculated from Eq. (22), using the magnitudes of the coefficients  $a$  and  $b$  obtained from the best fit to the  $\omega_{co}(H)$  data based on Eq. (22); i.e.,  $\omega_{co}(0) = a(1 + b)$ . The  $\omega_{co}(0, p)$  or  $\omega_{co}(0, p')$  data, so obtained, obey the power law, Eq. (21), with the same value of  $p_c$  or  $p'_c$  as that mentioned above but with the exponent  $\theta_p + 2\nu_p = 3.23(3)$  for both alloy series. That Eq. (21) [Eq. (22)] does indeed describe the concentration [field] dependence of  $\omega_{co}(0)$  [ $\omega_{co}(H)$ ] for the alloys in question is clearly demonstrated by the data presented in figure 5 [Fig. 7]. Since the quantity of interest in the theory is  $\omega_{co}(0)$  and not  $\omega_{co}(H)$ , the values of the exponent for  $\omega_{co}(0)$  and  $\theta_p$  are used to arrive at the result  $\nu_p = 0.89(3)$ . Moreover, the relation<sup>15</sup>  $\theta_p = \sigma_p - \beta_p$  [where  $\sigma_p$  is the conductivity percolation critical exponent, defined as<sup>1,3</sup> macroscopic conductivity  $\Sigma \sim (p - p_c)^{\sigma_p}$ ] and Eq. (16) yield  $\sigma_p = 1.86(4)$  and  $D_f = 2.54(3)$ . The estimates for the percolation critical exponents  $\beta_p, \theta_p, \nu_p, \sigma_p$ , thermal-to-percolation crossover

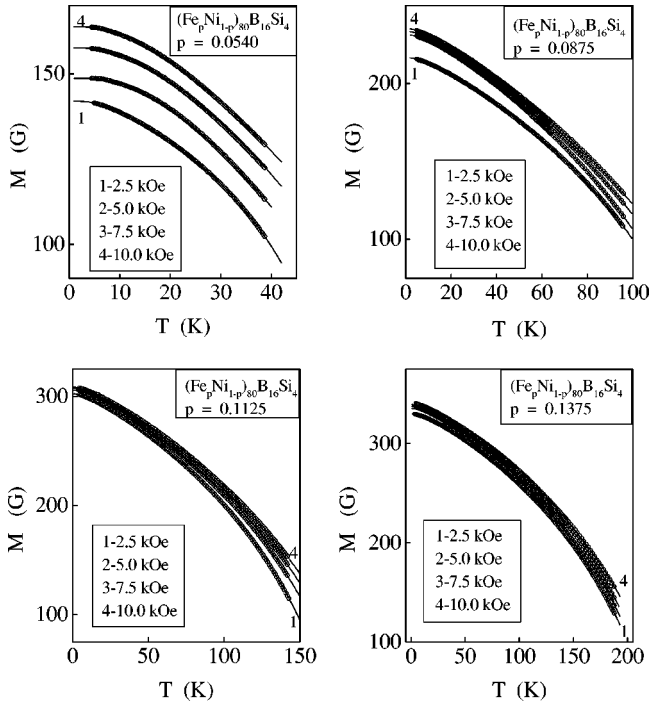


FIG. 4. Temperature variations of magnetization at fixed magnetic fields  $H=2.5, 5.0, 7.5,$  and  $10.0$  kOe for  $a-(\text{Fe}_p\text{Ni}_{1-p})_{80}\text{B}_{16}\text{Si}_4$  alloys. The solid curves through the data points are the best least-squares fits to the  $M(T, H)$  data based on Eqs. (15), (17), and (18) of the text. The experimental and theoretical variations of magnetization with temperature are typical of those found in  $a-(\text{Co}_p\text{Ni}_{1-p'})_{80}\text{B}_{16}\text{Si}_4$  alloys as well.

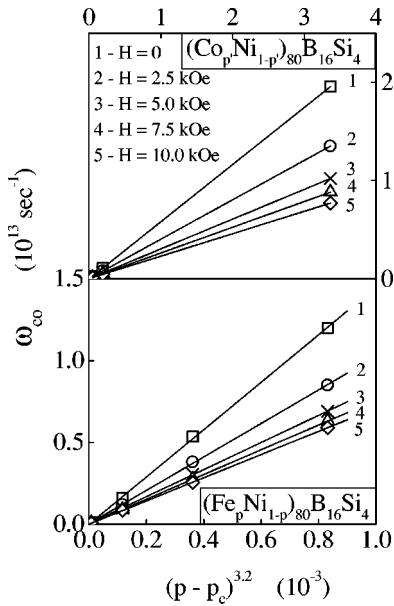


FIG. 5. The lower (upper) panel of the figure displays Fe (Co) concentration  $p$  ( $p'$ ) dependence of the crossover frequency ( $\omega_{co}$ ) at different but fixed values of field ( $H$ ). The straight lines through the data points represent the optimum fits to the  $\omega_{co}(0, p)$  or  $\omega_{co}(H, p)$  data based on Eq. (21) of the text.

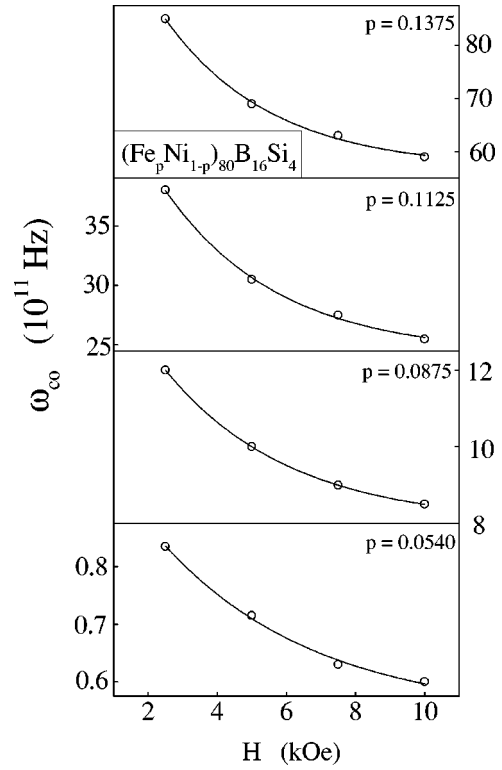


FIG. 6. Variation of the crossover frequency  $\omega_{co}$  with field  $H$  for  $a-(\text{Fe}_p\text{Ni}_{1-p})_{80}\text{B}_{16}\text{Si}_4$  alloys. The curves through the data points (open circles) are the best least-squares fits based on Eq. (22) of the text. The experimental and theoretical variations of  $\omega_{co}$  with field are typical of those found in the  $a-(\text{Co}_p\text{Ni}_{1-p'})_{80}\text{B}_{16}\text{Si}_4$  alloys as well.

exponent  $\phi$ , and fractal dimension  $D_f$  obtained either directly or with the aid of exponent equalities conform very well with those predicted by the theory.<sup>1,3</sup> Such an agreement asserts that quenched randomness does not alter the critical behavior of percolation on a regular  $d=3$  lattice. While the result  $\tilde{d}_f = 1.33(3)$  vindicates the Alexander-Orbach conjecture,<sup>2</sup> the finding  $\sigma_p < 2$  is consistent with the Golden inequality.<sup>16</sup>

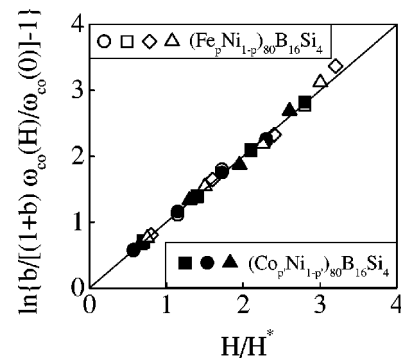


FIG. 7. Scaling of the quantity  $\ln\{b/[(1+b)\omega_{co}(H)/\omega_{co}(0)]-1\}$  with reduced field  $H/H^*$  for all the compositions in the amorphous alloy series  $(\text{Fe}_p\text{Ni}_{1-p})_{80}\text{B}_{16}\text{Si}_4$  and  $(\text{Co}_p\text{Ni}_{1-p'})_{80}\text{B}_{16}\text{Si}_4$ . This scaling form is based on Eq. (22) of the text.

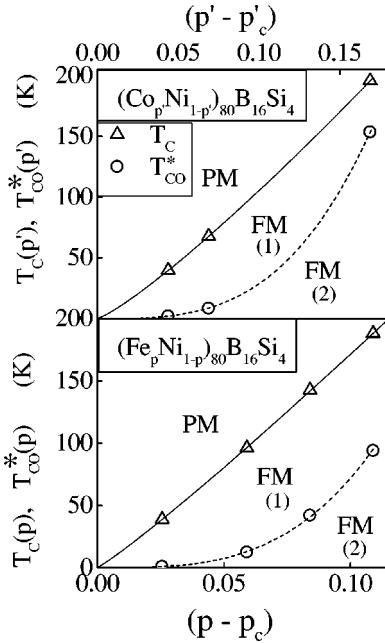


FIG. 8. Magnetic phase diagrams for the amorphous alloy series in question that display the two crossover lines: the thermal-to-percolation crossover or the paramagnetic (PM) to ferromagnetic (FM) phase transition,  $T_c(p)$ , line (solid curve) and the hydrodynamic-to-critical spin wave crossover, or the magnon-to-fracton crossover,  $T_{co}^*(p)$ , line (dashed curve) within the FM phase.

$\omega_{co}(0)$  permits determination of the temperature  $T_{co}^* = \hbar \omega_{co}(0)/k_B$  at which the crossover from the hydrodynamic regime to the critical regime occurs. The locus of  $T_{co}^*$  values for different compositions in a given alloy series is the crossover line (dashed curve) that divides the *ordered* (ferromagnetic) FM phase into two regions (1) and (2) in the magnetic phase diagrams shown in Fig. 8. In region (2), thermal demagnetization is solely due to hydrodynamic spin waves whereas in region (1) both hydrodynamic and critical magnons (ferromagnetic fractons) are responsible for the decline of spontaneous magnetization with increasing temperature. This crossover line occurs at lower temperatures and is in addition to the thermal-to-percolation crossover line (solid curve), i.e., the phase boundary between the *disordered* [paramagnetic (PM)] phase and *ordered* (FM) phase.

We conclude the discussion of results with a few remarks about a possible contribution to  $M(T, H)$  due to *finite* ferromagnetic clusters. The only effect of the magnetic field  $H$  considered in this work is the *increase* in the percolation correlation length  $\xi_0(p)$  [and hence *decrease* in the crossover frequency  $\omega_{co}$  in Eq. (15)] and the suppression of spin waves (thermally excited in the *infinite* ferromagnetic cluster or network) through a gap in the spin-wave spectrum, Eq. (17). However, the field  $H$  is also expected to align the magnetizations of finite clusters along its own direction and thereby affect the dependences on  $T$  and  $H$  of the overall magnetization. For dilute ferromagnets with composition ( $p$ ) in the close proximity to the percolation threshold ( $p_c$ ), finite ferromagnetic spin clusters with a broad size distribution

coexist<sup>17</sup> with infinite ferromagnetic network. As  $p$  is increased above  $p_c$ , the infinite ferromagnetic network grows at the expense<sup>17</sup> of finite ferromagnetic clusters whose number reduces<sup>17</sup> rapidly and size distribution narrows down.<sup>17</sup> The finite spin clusters interact with one another through *weak* long-range Ruderman-Kittel-Kasuya-Yosida (RKKY) interactions and at low temperatures freeze in random orientations so that below a certain temperature  $T_{RE}$  a (reentrant) *mixed* state is formed in which long-range ferromagnetic order (i.e., infinite ferromagnetic network) coexists<sup>17,18</sup> with cluster spin glass order. Especially for concentrations  $p \approx p_c$ ,  $T_{RE}$  is very close to, but below, the Curie temperature  $T_C$  and for  $T < T_{RE}$  the finite spin clusters, frozen in random orientations, give rise to a sizable *local* random anisotropy (this anisotropy, however, cannot destroy<sup>17,18</sup> long-range ferromagnetic order in the infinite spin cluster because the coupling between the infinite cluster and finite clusters is weak). Consequently, the external magnetic field  $H$  has to work against a large anisotropy field to alter the orientations of finite-cluster magnetizations. In other words, extremely large magnetic fields are required to saturate magnetization in ferromagnets with  $p \approx p_c$ . This inference is consistent with our observations based on the  $M-H$  isotherms taken at 3.8 K. Moreover, very high temperatures ( $T \gg T_C$ ) are needed to excite spin waves within the finite ferromagnetic clusters as their *local* Curie temperatures lie well above the *bulk* Curie temperature of the infinite cluster. Thus a significant contribution to  $M(T, H)$  from finite spin clusters is expected only for dilute ferromagnets with  $p \approx p_c$  at high temperatures ( $T > T_C$ ) where the thermal energy is high enough to set the finite clusters free and excite intracluster spin waves. For the reasons stated above, such a contribution to  $M(T, H)$  has been completely ignored in the present case where Eqs. (15) and (17) have been used in the temperature range  $T \leq T_C$ .

#### IV. SUMMARY

High-resolution magnetization  $M(T, H)$  data have been taken on well-characterized amorphous  $(Fe_p Ni_{1-p})_{80} B_{16} Si_4$  and  $(Co_{p'} Ni_{1-p'})_{80} B_{16} Si_4$  alloys with composition ( $p, p'$ ) in the vicinity of the percolation threshold for the appearance of the long-range ferromagnetic order. An elaborate data analysis yields the results that (i) allow an accurate determination of the hydrodynamic-to-critical spin-wave crossover line in the magnetic phase diagram, the percolation-to-thermal crossover exponent, fractal and fracton dimensionalities, the percolation critical exponents for magnetization, spin-wave stiffness, correlation length, and conductivity, (ii) clearly bring out the functional forms, i.e., Eqs. (18) and (22), of  $D(T)$  and  $\omega_{co}(H)$ , (iii) vindicate the Alexander-Orbach conjecture and the Golden inequality for  $d=3$  percolating networks, and (iv) permit us to conclude that quenched randomness does not alter the critical behavior of percolation on a regular  $d=3$  lattice.

#### ACKNOWLEDGMENT

One of the authors (S.N.K.) is grateful to Professor H. Kronmüller for permitting the use of a SQUID magnetometer.

\*Electronic address: kaulsp@uohyd.ernet.in

- <sup>1</sup>T. Nakayama, K. Yakubo, and R.L. Orbach., *Rev. Mod. Phys.* **66**, 381 (1994) and references cited therein.
- <sup>2</sup>S. Alexander and R. Orbach, *J. Phys. (France) Lett.* **43**, L625 (1982).
- <sup>3</sup>D. Stauffer and A. Aharony, *Introduction to Percolation Theory* (Taylor & Francis, Bristol, 1991).
- <sup>4</sup>M.B. Salamon and Y. Yeshurun, *Phys. Rev. B* **36**, 5643 (1987).
- <sup>5</sup>K. Zadro, *J. Magn. Magn. Mater.* **163**, L5 (1996).
- <sup>6</sup>R.B. Stinchcombe and I.R. Pimentel, *J. Phys. A* **21**, L807 (1988).
- <sup>7</sup>H. Ikeda, J.A. Fernandez-Baca, R.M. Nicklow, M. Takahashi, and K. Iwasa, *J. Phys.: Condens. Matter* **6**, 10543 (1994) and references cited therein.
- <sup>8</sup>S. Srinath, S.N. Kaul, and M.-K. Sostarich, *Phys. Rev. B* **62**, 11 649 (2000).
- <sup>9</sup>S.N. Kaul, *IEEE Trans. Magn.* **17**, 1208 (1981).
- <sup>10</sup>S. Srinath, S. N. Kaul, and M.-K. Sostarich, in *Proceedings of the DAE Solid State Physics Symposium* (BARC, Mumbai, India, 1996), Vol. 39C, p. 348.
- <sup>11</sup>S.N. Kaul and P.D. Babu, *Phys. Rev. B* **50**, 9323 (1994).
- <sup>12</sup>A. Aharony, S. Alexander, O. Entin-Wohlman, and R. Orbach., *Phys. Rev. B* **31**, 2565 (1985); A. Aharony, O. Entin-Wohlman, S. Alexander, and R. Orbach, *Philos. Mag. B* **56**, 949 (1987).
- <sup>13</sup>E.F. Shender, *J. Phys. C* **9**, L309 (1976).
- <sup>14</sup>S.N. Kaul and P.D. Babu, *Phys. Rev. B* **50**, 9308 (1994).
- <sup>15</sup>S. Kirkpatrick, *Solid State Commun.* **12**, 2109 (1973).
- <sup>16</sup>K. Golden, *Phys. Rev. Lett.* **65**, 2923 (1990).
- <sup>17</sup>S.N. Kaul, *Solid State Commun.* **36**, 279 (1980); *IEEE Trans. Magn.* **20**, 1290 (1984); *J. Magn. Magn. Mater.* **53**, 5 (1985).
- <sup>18</sup>S.N. Kaul, *J. Phys.: Condens. Matter* **3**, 4027 (1991); S.N. Kaul, V. Siruguri, and G. Chandra, *Phys. Rev. B* **45**, 12 343 (1992), S.N. Kaul and P.D. Babu, *J. Phys.: Condens. Matter* **10**, 1563 (1998).